Subpiconewton Dynamic Force Spectroscopy Using Magnetic Tweezers

M. Kruithof, F. Chien, M. de Jager, and J. van Noort
Leiden Institute of Physics, 2333 CA Leiden, The Netherlands

ABSTRACT   We introduce a simple method for dynamic force spectroscopy with magnetic tweezers. This method allows application of subpiconewton force and twist control by calibration of the applied force from the height of the magnets. Initial dynamic force spectroscopy experiments on DNA molecules revealed a large hysteresis that is caused by viscous drag on the magnetic bead and will conceal weak interactions. When smaller beads are used, this hysteresis is sufficiently reduced to reveal intramolecular interactions at subpiconewton forces. Compared with typical quasistatic force spectroscopy, a significant reduction of measurement time is achieved, allowing the real-time study of transient structures and reaction intermediates. As a proof of principle, nucleosome-nucleosome interactions on a subsaturated chromatin fiber were analyzed.

INTRODUCTION

To probe the mechanics of biomolecules at the single-molecule level, a variety of force microscopy techniques have been developed such as optical tweezers (OT), magnetic tweezers (MT), and atomic force microscopy (AFM) (1). With these techniques, the energy landscape of biological bonds can generally be resolved accurately by applying an increasing force to a molecule and measuring its extension in time. Evans and Ritchie (2) showed that careful analysis of the rupture force as a function of the force-loading rate reveals both the interaction distance and the energy barrier of a molecular bond. The energy dissipated by the rupture can be quantified from the hysteresis in a force-distance (F-D) cycle. OT and AFM are well suited for such dynamic force spectroscopy experiments, as they both combine a position trap with nanometer resolution manipulation. However, the high spring constants of these traps in combination with the ever-present Brownian fluctuations limit the force accuracy of these techniques to ~1 pN for OT and 10 pN for AFM.

In contrast, MT, which consist of a pair of permanent magnets in combination with a paramagnetic bead, can be characterized as force clamps because they do not fix the position of the trapped bead but the applied force. The effective stiffness of the trap depends on the compliance of the polymer that tethers the bead to the surface. The applied force is calculated from the Brownian motion of the bead using equipartition theory. As a consequence of the high compliance of the tether, forces down to 10 fN are experimentally accessible, as shown, for example, by Strick et al. (3). MT also clamp and constrain the rotation of the bead, giving a unique handle on, for example, DNA topology. These features have made MT an indispensable tool to reveal many of the mechanical properties of DNA and DNA-interacting proteins such as topoisomerases, helicases, and chromatin remodelers (4). Unfortunately, as a consequence of the small effective spring constant of these molecules at small forces and the large viscous damping of the bead, accurate quantification of the Brownian motion is time consuming and extends up to tens of minutes per force point. As a consequence, MT can typically be operated only in a quasistatic force mode, where a series of force points needs to be acquired to obtain a full F-D profile (5).

In this article we introduce dynamic force spectroscopy for MT. Here the magnetic force is calibrated to the magnet position. From this relation the applied force is calculated while the bead position is detected in real time. A major advantage of dynamic force spectroscopy using MT compared with OT and AFM is that a sub-pN range of forces become accessible that are relevant in many biological applications. Moreover, measurement times are reduced by two orders of magnitude compared with traditional quasistatic force spectroscopy. This strong reduction of measurement time significantly relieves instrumentation drift issues commonly associated with MT experiments. Transient interactions that readily dissociate on extended periods of increased force can now be measured with the highest accuracy. The artifacts that are caused by the dominant role of Brownian motion at low forces, as well as the relatively high viscous drag on the bead, are discussed and resolved.

MATERIALS AND METHODS

Magnetic tweezers

DNA-tethered paramagnetic beads were imaged in a home-built inverted microscope with a CCD camera (Pulnix TM-6710CL, Copenhagen, DK) at 60 frames per second. The magnet position was controlled by a stepper motor-based translation stage (M-126, Physik Instrumente, Karlsruhe, Germany) with an accuracy of 200 nm. The position of the beads was measured by real time image processing using LabView software (National Instruments, Austin, TX) with an accuracy of 10 nm. A schematic layout of the experimental geometry is shown in Fig. 1. During a quasistatic force measurement, the force at each magnet position was calculated from the
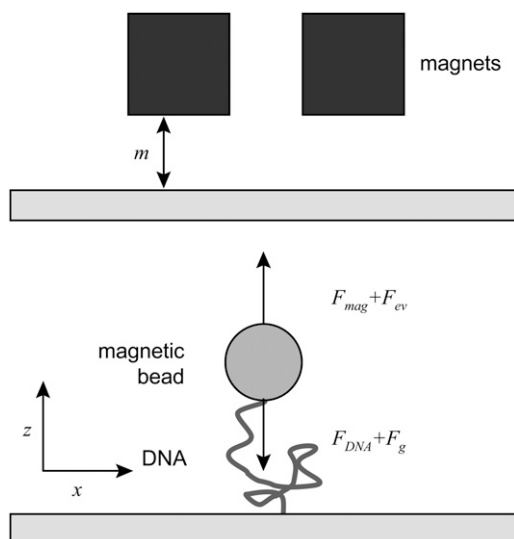
FIGURE 1 Schematic layout of the experimental geometry. The forces pulling the bead up are the magnetic force, F_{mag}, and the force resulting from excluded volume effects, F_{ev}. The gravitational force, F_g, and the force applied by the DNA, F_{DNA}, pull the bead downward. The dimensions of the drawing are not to scale.

fluctuations of the bead in the transverse direction, x, parallel to the coverslip and from the average height of the bead, z, normal to the coverslip (3):

$$F = k_B T \frac{\langle z(t) \rangle}{\langle (\bar{x} - x(t))^2 \rangle}. \tag{1}$$

During a dynamic force measurement, the magnets were moved toward the bead and back at a constant speed, resulting in a forward and backward trace, respectively. The position of the magnets was calculated from the position of the stepper motor.

Magnetic beads

Paramagnetic tosylactivated Dynabeads (Invitrogen, Carlsbad, CA) were coated with antidigoxigenin antibodies (Sigma, St. Louis, MO) according to the protocol suggested by the supplier.

Sample preparation

A clean glass coverslip was coated with a 10 μg/ml poly-d-lysine solution (Sigma). Next, the coverslip was incubated with a polyethyleneglycol (PEG) solution containing a mixture of 20% w/v mPEG-succinimidyl propionic acid (SPA)-5000 and 0.2% biotin-PEG-N-hydroxysuccinimide (NHS)-3400 (Nektar, San Carlos, CA) in sterile filtered 0.1 M NaHCO$_3$ buffer (pH 8.5) for 3 h at room temperature. The coverslip was then mounted on a poly-dimethylsiloxane (PDMS) flowcell containing a $10 \times 40 \times 0.4$ mm flow channel and flushed with 1 ml measurement buffer MB (10 mM HEPES, pH 7.6, 100 mM KAc, 2 mM MgAc, 10 mM NaN$_3$, and 0.1% (v/v) Tween-20 in milli-Q water). Next, 0.1 mg/ml streptavidin (Sigma) was flushed into the cell and incubated for 10 min. The cell was subsequently flushed with 1 ml of MB, 400 μl 2.5 ng/μl DNA in MB and incubated for 10 min, 1 ml MB, 1 μl magnetic beads in 400 μl MB supplemented with 0.02% (w/v) bovine serum albumin (MB+) and incubated for 10 min and finally flushed with MB+.

DNA and chromatin fibers

A construct of pBlueScript SK+ with a cloned insert containing 17 5S RNA nucleosome positioning sites was digested with HindIII and NotI. The

fragment containing 17 positioning elements was purified, and 1300-base-pair (bp) PCR fragments (template: pBluescript K+; primers: 5′-CTA-AATTGTAAGCGTTAATATTTTGTTAAA-3′ and 5′-TATCTTTATA-GTCCTGTCGGGTTTCGCCAC-3′) containing either digoxygenin- or biotin-modified uracils in a ratio of 1:20 to nonmodified thymine were digested with Not I and HindIII, respectively. The resulting ~650-bp fragments were ligated, with an excess of 10:1, to each end of the vector fragment carrying the 17 positioning elements and used without further purification. Electrophoretic gel analysis showed that all the vector fragments were ligated to the linker fragments. For nucleosome reconstitution, a salt dialysis with recombinant histone proteins was performed as described elsewhere (6). The histone octamer/positioning site ratio was 1:1, but the yield of reconstitution was significantly less.

AFM

Subsaturated chromatin fibers were imaged with tapping mode AFM on a Nanoscope III (Veeco, Woodbury, NY) after glutaraldehyde fixation and deposition on mica.

RESULTS AND DISCUSSION

Validation of the method

To empirically determine the relation between force and magnet position, we performed quasistatic force measurements on single DNA molecules. A typical result of these measurements is shown in Fig. 2 a. The F-D plot accurately follows the worm-like chain (WLC) (7)

$$F_{DNA}(z) = \frac{k_B T}{p} \left\{ \frac{1}{4(1 - z/L_0)^2} - \frac{1}{4} + \frac{z}{L_0} \right\} \tag{2}$$

with thermal energy $k_B T$, extension z, fitted persistence length $p = 48$ nm, and contour length $L_0 = 1.26$ μm. In Fig. 2 b we plotted the force obtained as a function of the magnet position. We found that the force F_{tot} decays exponentially with the magnet position, according to

$$F_{tot} = F_{mag,0} \, e^{-m/b} + F_0, \tag{3}$$

where m is the distance between the top of the fluidic cell and the magnets as depicted in Fig. 1. $F_{mag,0}$ is the maximal force, b the decay length of the magnetic force, and F_0 a constant offset. In our setup $F_{mag,0}$ was 18 ± 2 pN for 2.8-μm-diameter beads and 6 ± 1.4 pN for 1-μm-diameter beads. We found the decay length, which is defined by the geometry of the setup, to be constant, $b = 1.1 \pm 0.07$ mm. Below 100 fN, the observed force is independent of the magnet position. In this regime excluded-volume effects, pushing the bead away from the surface and gravity, pulling the bead down, dominate (8). We estimated F_0, the sum of the forces originating from gravity and excluded volume effects, to be ~31 fN, in good agreement with a fitted offset of 27 fN. During a dynamic force measurement Eq. 3 was used to calculate the force from the magnet position.

To test the dynamic force mode, we acquired a F-D cycle on a DNA molecule shown in Fig. 3 a. Each forward-pulling trace was acquired in 5 s, and the backward trace was acquired at the same speed. Note that this is much shorter than a quasistatic measurement like the one shown in Fig. 2 a, which was
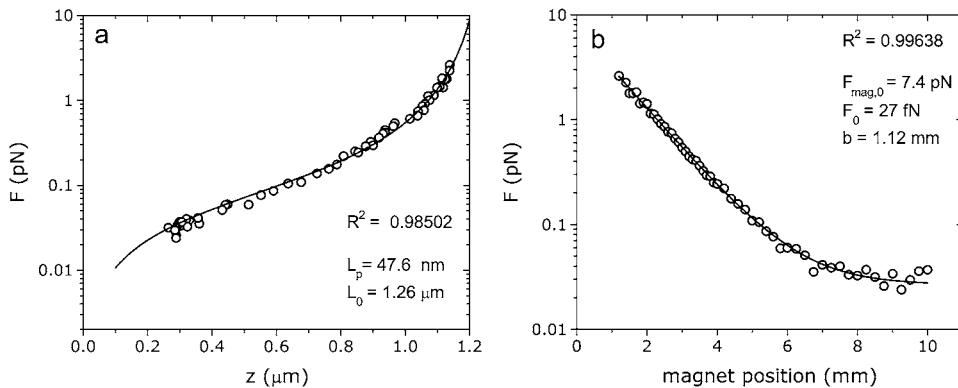
FIGURE 2 Force calibration for dynamic force spectroscopy. (*a*) A F-D plot of a DNA molecule obtained with quasistatic force spectroscopy (*solid circles*) fits the WLC model (*solid line*). (*b*) The force at different magnet positions (*solid circles*) follows an exponential decay with an additional offset (*solid line*).

measured in ~1 h. Surprisingly, significant hysteresis was observed between the forward (increasing force) and backward (decreasing force) trace. When this trace was compared with the WLC fit obtained with quasistatic force spectroscopy, it appeared that both the forward and the backward trace follow the WLC only at forces above 1 pN. At forces below 1 pN, however, only the backward trace matches the WLC curve. Because DNA has been shown to deform elastically at forces below its melting transition, i.e., below 60 pN (5), the origin of this hysteresis cannot be internal disruption of the DNA structure and must therefore be attributed to external dissipation.

Nonspecific interactions of the DNA and/or bead with the surface are commonly observed in these measurements, especially at low forces and might alternatively explain the observed behavior. Disruption events of such nonspecific interactions are generally accompanied by a movement in the lateral direction, as shown in Supplementary Fig. 1. To discriminate between surface interactions and intramolecular interactions, we used the absence of lateral movement as a selection criterion. Furthermore, after PEG passivation no F-D cycles on DNA and only a small fraction of F-D cycles on chromatin showed lateral movement. Thus, nonspecific
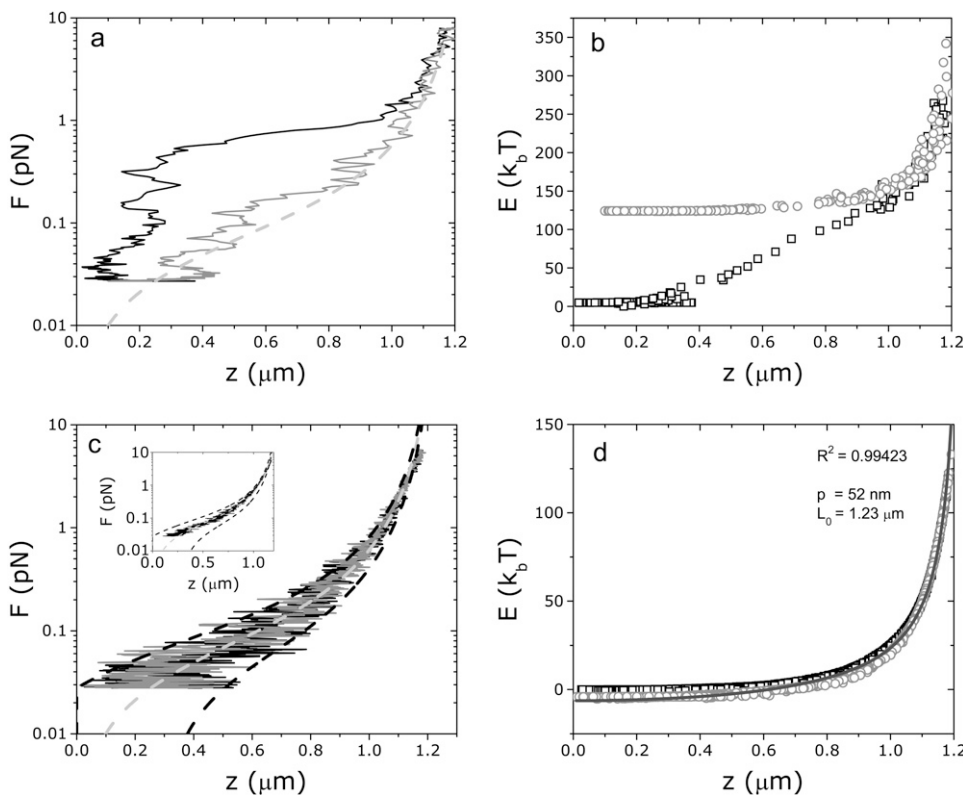

FIGURE 3 Dynamic force spectroscopy on DNA using large and small magnetic beads. (*a*) Dynamic force spectroscopy using 2.8-μm beads. The forward trace (*solid line*) and backward trace (*shaded line*) do not overlap, indicating energy dissipation; the dashed light gray line is a WLC with a persistence length of 52 nm and a contour length of 1.2 μm. Each trace was obtained in 5 s. (*b*) The work during the experiment as a function of the extension. The forward trace (*squares*) and backward trace (*circles*) do not overlap, indicating dissipation. (*c*) Dynamic force spectroscopy using 1-μm beads. The forward trace (*solid line*) and backward trace (*shaded line*) overlap. The dashed black line is a WLC with the persistence length and contour length taken from the fit in *d*. The dashed black lines are the expected standard deviation of the Brownian noise of the bead as can be calculated from Eq. 2. The inset shows the average of six traces (*solid line*); the noise in the traces is clearly reduced. Each trace was obtained in 5 s. (*d*) The work during the experiment as a function of the extension; the forward trace (*squares*) and backward trace (*circles*) overlap, indicating a fully elastic response. A WLC model was fitted to the backward trace (*solid line*).

interactions between the tether and the surface can be discarded as the origin of the hysteresis.

Understanding the nature of the observed hysteresis is a requirement for F-D analysis of more complex structures. Therefore, we considered the equation of motion of the tethered bead, which is given by the Langevin equation

$$F_{DNA}(z) = F_{mag} - \gamma \frac{dz}{dt} \qquad (4)$$

with z the position of the bead and γ the drag coefficient. Inertia forces can readily be neglected. Rapid changes in magnetic force will induce an extra friction force that makes the bead lag behind. The friction coefficient γ is given by Stokes' law

$$\gamma = 6\pi \eta r \qquad (5)$$

with bead radius r and viscosity η. Note that the viscosity at close proximity to the surface, η^*, can be significantly larger than the bulk viscosity when the radius of the bead, r, is comparable to the distance between the bead and the coverslip, z (9):

$$\eta^* = \left(1 + \frac{r}{z} + \frac{r}{6z + 2r}\right)\eta. \qquad (6)$$

During a dynamic force measurement, we assumed that the force on the molecule is equal to the applied magnetic force determined in a quasistatic measurement. However, from Eq. 4, it is clear that friction also contributes to the applied force, $F_{fr} = \gamma(dz/dt)$. The relative contribution of the friction, F_{fr}/F_m, can be rewritten to

$$\frac{F_{fr}}{F_m} = 6\pi \frac{brv_{mag}\eta}{k} \qquad (7)$$

with v_{mag} the velocity of the magnets and k the spring constant of the tether. In the case of DNA, the viscous drag is most limiting in the entropic regime, where DNA behaves as a Hookian spring with $k = (3/2)(k_B T/pL_0)$, resulting in the following formula for the relative contribution of the friction:

$$\frac{F_{fr}}{F_m} = \frac{12}{3}\pi \frac{bprv_{mag}L_0\eta}{k_b T}. \qquad (8)$$

The assumption that the force on the molecule is equal to the applied magnetic force is valid only when the friction force is negligible compared with the magnetic force ($F_{fr}/F_m \ll 1$). The maximum magnet velocity typically used in experiments was 2 mm/s. For 2.8-μm-diameter beads, $F_{fr}/F_m = 0.43$, which is clearly not negligible. Decreasing the bead diameter will decrease this contribution. For example, the contribution of friction to the total force on 1-μm-diameter beads is much smaller ($F_{fr}/F_m = 0.15$) and will lead to a more accurate F-D curve as quantified in the next paragraph. A dynamic F-D plot measured using a 1-μm-diameter bead is shown in Fig. 3 c. In contrast to the data obtained with 2.8-μm-diameter beads (Fig. 3 a), the data follow the WLC model accurately, and no obvious hysteresis was observed between the forward and the backward trace.

Energy analysis

Brownian motion of the bead causes the large fluctuations in the low-force regime as demonstrated in Fig. 3 a, making it difficult to assess any residual dissipation. Averaging of Brownian fluctuations from multiple F-D curves reduces this effect, as shown in Fig. 3 c, inset. However, averaging precludes the ability to resolve single ruptures that are not synchronous in repeated experiments, a major advantage of dynamic force spectroscopy. As an alternative, we calculated the work done during a single F-D cycle, i.e., $E(t) = F \int_0^t dt^* (dz/dt^*)$, which results in an energy-distance (E-D) plot as shown in Fig. 3 d. Because the Brownian motion is now integrated, all fluctuations will collapse on the curve

$$E(z) = \int_0^z F_{DNA}dz = \frac{1}{4}\frac{k_B T\, z^2(2z - 3L_0)}{p L_0(z - L_0)}. \qquad (9)$$

Both the forward and backward trace fit very well to Eq. 9 for $p = 49$ nm and $L_0 = 1.18$ μm.

From the measurements we also obtained the total dissipated energy, $\Delta E = F \int dt(dz/dt)$ in a single F-D cycle, which manifests itself as hysteresis in the F-D plot. After a full F-D cycle, the dissipation was $\sim$3 $k_B T$ for 1-μm-diameter beads, compared with 130 $k_B T$ for measurements with 2.8-μm-diameter beads. Alternatively, an increase of the measurement time for each trace, from 5 to 60 s, decreased the hysteresis on a 2.8-μm bead (data not shown) and resulted in a dissipation of 6 $k_B T$. These values are in close agreement with numerical solutions of Eqs. 4–6, for DNA with a contour length of 1.2 μm, a persistence length of 52 nm, and a measurement time corresponding to 5 s. For a dynamic F-D experiment, these calculations resulted in a dissipation of 147 $k_B T$ for 2.8-μm-diameter beads and 3 $k_B T$ for 1-μm-diameter beads.

From these experiments, we can conclude that when smaller magnetic beads are used: 1), dissipation from viscous drag is negligible; i.e., the molecule is permanently in equilibrium with the magnetic force; 2), nonspecific interactions of the bead and/or DNA with the surface were negligible; and 3), DNA extension is fully elastic at forces down to 10 fN.

In the current measurements, the force was increased exponentially in time, effectively emphasizing the low-force regime. With a more advanced, nonlinear control of the magnet position, one could also linearly ramp the force, making low-force dynamic force spectroscopy MT experiments possible that are compatible with the framework developed for previous studies (2).

Dynamic force spectroscopy on nucleosome-nucleosome interactions

In eukaryotes, DNA is condensed into chromatin. Although the structure of the nucleosome, the first step in DNA condensation, is known with atomic precision (10), higher-order structures remain highly elusive (11). Full understanding of

higher-order structure and dynamics will require detailed knowledge of all interactions among the nucleosomes. However, only rough estimates of the interaction energy are currently available because of a lack in force accuracy and the common use of chromatin reconstituted from highly heterogeneous cell extracts (12). We recently obtained well-defined, fully saturated chromatin fibers that adopt a 30-nm fiber structure (13). These extremely well-ordered structures are stabilized by multiple nucleosome-nucleosome interactions that act in concert. Such 30-nm fibers, when measured using dynamic force spectroscopy as described in this article, resist forces up to 4.5 pN, after which the structure unfolds cooperatively. Because of the cooperative nature of unfolding, individual interactions between nucleosomes were completely obscured in these experiments (M. Kruithof, F. Chien, A. Routh, D. Rhodes, C. Logie, and J. van Noort, unpublished data). To resolve individual nucleosome-nucleosome interactions, we did dynamic force spectroscopy on individual subsaturated chromatin fibers in which nucleosomes can interact but are too sparse to adapt highly condensed structures.

AFM imaging of the subsaturated chromatin fibers reveals a large variation of the number and position of nucleosomes on each DNA template molecule, with an average number of nucleosomes per molecule of 4 ± 3, as shown in Fig. 4 *a*. Some of the nucleosomes interact, causing looping of the DNA as indicated by the arrow. In Fig. 4, *b* and *c*, F-D and

E-D plots of a measurement on a single subsaturated chromatin fiber are shown. Compared with bare DNA (Fig. 3 *c*), the tether extension is significantly reduced. At an applied force of ~0.5 pN, the structure ruptured to an extended length, after which the forward and backward traces overlap. In the E-D plot, we observed a total energy dissipation of 20 k_BT that we attributed to the rupture of nucleosome-nucleosome interactions. The dissipated energy varied significantly between F-D cycles, pointing at different interactions in each refolding cycle.

After rupture of the interactions between nucleosomes, the DNA is expected to follow the WLC model, having a reduced contour length because of DNA wrapping in nucleosomes and a reduced persistence length as a result of the sharp bends at the entry and exit sites of a nucleosome (14). Indeed, the backward trace in Fig. 4 *c* fits well to Eq. 9, with $L_0 = 0.89$ μm and $p = 18$ nm. It is clear that because these two effects are correlated, a smaller contour length indicates more nucleosomes resulting in a smaller persistence length. From the amount of wrapped DNA, 310 nm, it follows that this fiber contained six nucleosomes. The results obtained for several molecules were further analyzed, Fig. 4 *d*. As expected, a clear correlation between the resulting contour length and persistence length was observed. For a quantitative comparison of these traces, we divided the traces into two populations, the first with a contour length >1 μm, containing very few or no nucleosomes, and the second with a contour
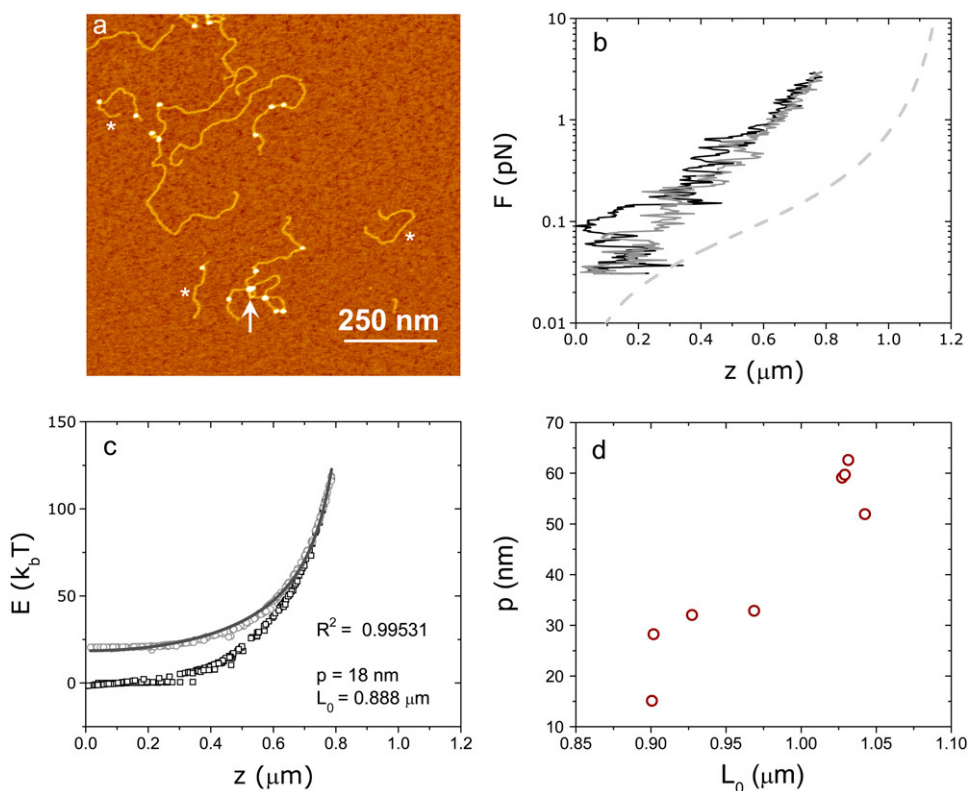

FIGURE 4 Dynamic force spectroscopy on subsaturated chromatin fibers. (*a*) AFM image of the chromatin fibers used. Possible nucleosome-nucleosome interactions are indicated by an arrow. Stars denote PCR fragments used in the MT for linking the fiber to the bead and the surface. (*b*) Dynamic force spectroscopy on these chromatin fibers. The forward trace (*solid line*) and backward trace (*shaded line*) do not overlap at forces <1 pN. The dashed light gray line is a WLC with a persistence length of 52 nm and a contour length of 1.2 μm, appropriate for a bare DNA tether. Each trace was obtained in 5 s. (*c*) The work during the experiment as a function of the extension. The forward trace (*squares*) and backward trace (*brown circles*) do not overlap and show an offset that can be attributed to disruption of nucleosome-nucleosome contacts. The backward trace closely follows the WLC model (*solid line*). (*d*) The fitted contour length of different subsaturated chromatin fibers plotted versus the fitted persistence length.

length <1 μm, containing more than four nucleosomes. We averaged the persistence length, contour length, and dissipated energy over the traces within each population. The persistence length differed significantly between the two populations: 27 ± 8 nm and 58 ± 5 nm, respectively. The average dissipated energy was higher for the population with the smaller contour length (16 ± 8 k_BT vs. 10 ± 6 k_BT). However, the variations in dissipated energy are large, especially in the case with the greater number of nucleosomes. This can be expected because these unstructured arrays can adopt different nucleosome-nucleosome interactions in each F-D cycle.

Recently, Mihardja et al. reported the unwrapping of DNA within a single nucleosome at forces between 2 and 4 pN (15). At comparable pulling rates, we did not observe any unwrapping of the DNA from the nucleosomes up to forces of 6 pN. When the magnets were positioned to apply a maximum force for an extended period of time, we did observe unwrapping, as plotted in Supplementary Fig. 1 *c*, showing that we can use dynamic force spectroscopy to study transient structures that have a limited lifetime under an applied load.

CONCLUSION

In conclusion, we developed a method for fast real-time subpiconewton dynamic force spectroscopy using MT. We showed that the energy dissipation from viscous drag is dependent on bead diameter. The large Brownian fluctuations of the bead position that occur at low forces conveniently collapse on a well-defined energy-distance plot, allowing accurate analysis of dynamic force spectroscopy data and calculation of the dissipated energy. As a proof of principle, measurements on single subsaturated chromatin fibers revealed a clear correlation between contour length and persistence length. Nucleosome-nucleosome interactions that rupture at 0.5 pN with a dissipated energy in the range of 10–16 k_BT were observed.

SUPPLEMENTARY MATERIAL

To view all of the supplemental files associated with this article, visit www.biophysj.org.

REFERENCES

1. Clausen-Schaumann, H., M. Seitz, R. Krautbauer, and H. E. Gaub. 2000. Force spectroscopy with single bio-molecules. *Curr. Opin. Chem. Biol.* 4:524–530.

2. Evans, E., and K. Ritchie. 1997. Dynamic strength of molecular adhesion bonds. *Biophys. J.* 72:1541–1555.

3. Strick, T. R., J. F. Allemand, D. Bensimon, A. Bensimon, and V. Croquette. 1996. The elasticity of a single supercoiled DNA molecule. *Science.* 271:1835–1837.

4. Zlatanova, J., and S. H. Leuba. 2003. Magnetic tweezers: a sensitive tool to study DNA and chromatin at the single-molecule level. *Biochem. Cell Biol.* 81:151–159.

5. Gosse, C., and V. Croquette. 2002. Magnetic tweezers: micromanipulation and force measurement at the molecular level. *Biophys. J.* 82:3314–3329.

6. Logie, C., and C. L. Peterson. 1997. Catalytic activity of the yeast SWI/SNF complex on reconstituted nucleosome arrays. *EMBO J.* 16:6772–6782.

7. Bustamante, C., J. Marko, E. Siggia, and S. Smith. 1994. Entropic elasticity of lambda-phage DNA. *Science.* 265:1599–1600.

8. Segall, D., P. Nelson, and R. Phillips. 2006. Volume-exclusion effects in tethered-particle experiments: bead size matters. *Phys. Rev. Lett.* 96:088306.

9. Bevan, M., and D. Prieve. 2000. Hindered diffusion of colloidal particles very near to a wall: Revisited. *J. Chem. Phys.* 113:1228–1236.

10. Luger, K., A. W. Mäder, R. K. Richmond, D. F. Sargent, and T. J. Richmond. 1997. Crystal structure of the nucleosome core particle at 2.8 a resolution. *Nature.* 389:251–260.

11. Tremethick, D. J. 2007. Higher-order structures of chromatin: the elusive 30 nm fiber. *Cell.* 128:651–654.

12. Cui, Y., and C. Bustamante. 2000. Pulling a single chromatin fiber reveals the forces that maintain its higher-order structure. *Proc. Natl. Acad. Sci. USA.* 97:127–132.

13. Huynh, V. A. T., P. J. J. Robinson, and D. Rhodes. 2005. A method for the in vitro reconstitution of a defined ''30 nm'' chromatin fibre containing stoichiometric amounts of the linker histone. *J. Mol. Biol.* 345:957–968.

14. Kulic, I. M., H. Mohrbach, V. Lobaskin, R. Thaokar, and H. Schiessel. 2005. Apparent persistence length renormalization of bent DNA. *Phys. Rev. E Stat. Nonlin. Soft Matter Phys.* 72:041905.

15. Mihardja, S., A. Spakowitz, Y. Zhang, and C. Bustamante. 2006. Effect of force on mononucleosomal dynamics. *Proc. Natl. Acad. Sci. USA.* 103:15871–15876.